



Published in final edited form as:

Nat Med. 2012 June ; 18(6): 956–960. doi:10.1038/nm.2758.

## A high throughput drug screen for *Entamoeba histolytica* identifies a new lead and target

Anjan Debnath<sup>1</sup>, Derek Parsonage<sup>2</sup>, Rosa M Andrade<sup>3,4</sup>, Chen He<sup>3</sup>, Eduardo R Cobo<sup>3</sup>, Ken Hirata<sup>3</sup>, Steven Chen<sup>5</sup>, Guillermina García-Rivera<sup>6</sup>, Esther Orozco<sup>6</sup>, Máximo B Martínez<sup>6</sup>, Shamila S Gunatilleke<sup>1</sup>, Amy M Barrios<sup>7</sup>, Michelle R Arkin<sup>5</sup>, Leslie B Poole<sup>2</sup>, James H McKerrow<sup>1</sup>, and Sharon L Reed<sup>3,4</sup>

<sup>1</sup>Sandler Center for Drug Discovery, University of California, San Francisco, California, USA

<sup>2</sup>Department of Biochemistry, Wake Forest School of Medicine, Winston-Salem, North Carolina, USA

<sup>3</sup>Department of Pathology, University of California, San Diego, California, USA

<sup>4</sup>Department of Medicine, University of California, San Diego, California, USA

<sup>5</sup>Small Molecule Discovery Center, University of California, San Francisco, California, USA

<sup>6</sup>Department of Experimental Pathology, CINEVESTAV-IPN, Mexico City, Mexico

<sup>7</sup>Department of Medicinal Chemistry, University of Utah, Salt Lake City, Utah, USA

*Entamoeba histolytica*, a protozoan intestinal parasite, is the causative agent of human amebiasis. Amebiasis is the fourth leading cause of death and the third leading cause of morbidity due to protozoan infections worldwide<sup>1</sup>, resulting in ~70,000 deaths annually. *E. histolytica* has been listed by the NIH as a category B priority biodefense pathogen in the United States. Treatment relies on metronidazole<sup>2</sup>, which has adverse effects<sup>3</sup> and potential resistance is an increasing concern<sup>4,5</sup>. To facilitate drug screening for this anaerobic protozoan, an automated, high-throughput screen (HTS) was developed and validated. Screening identified an FDA-approved drug, auranofin, used therapeutically for rheumatoid arthritis, as active against *E. histolytica* in culture (EC<sub>50</sub> 0.5 μM). Auranofin was 10-times more potent against *E. histolytica* than metronidazole. Transcriptional profiling and direct assays indicated that auranofin likely targets the *E. histolytica* thioredoxin reductase (EC<sub>50</sub> 0.4 μM), preventing the reduction of thioredoxin and enhancing sensitivity of trophozoites to reactive oxygen-mediated killing. In animal models of amebic colitis and liver abscess oral

Users may view, print, copy, download and text and data-mine the content in such documents, for the purposes of academic research, subject always to the full Conditions of use: [http://www.nature.com/authors/editorial\\_policies/license.html#terms](http://www.nature.com/authors/editorial_policies/license.html#terms)

Correspondence should be addressed to: S.L.R. (slreed@ucsf.edu) or A.D. (anjan.debnath@ucsf.edu).

### AUTHOR CONTRIBUTIONS

A.D. and J.H.M. designed the HTS screening studies, arrays, which A.D. performed. D.P. and L.B.P. performed the enzymatic assays. R.M.A. performed the oxidant studies. C.H., E.R.C., K.H., G.G.-R., E.O. and M.B.M. did the *in vivo* studies. K.H. purified r*Eh*TrxR. S.C. and M.R.A. provided compound libraries and edited the manuscript. S.S.G. and A.M.B. synthesized auranofin analogs. S.L.R. designed the *Eh*TrxR and oxidant studies. A.D., L.B.P., J.H.M. and S.L.R. wrote the manuscript.

### COMPETING FINANCIAL INTERESTS

The authors declare that they have no competing financial interest.

auranofin significantly reduced the number of parasites, the detrimental host inflammatory response, and hepatic damage. This new use of auranofin represents a promising therapy for amebiasis, and has been granted Orphan-Drug Status from the USFDA.

Screening large chemical libraries to identify amebicidals has been hindered by the throughput of traditional assays, which were labor intensive, relying on microscopic visualization<sup>6</sup>, radioisotopes<sup>7</sup>, and/or extensive staining methods<sup>8</sup>. We have developed and employed an automated HTS that is suitable for rapid and more efficient screening of large, diverse inhibitor libraries for activity against *E. histolytica*. The challenges for developing the HTS platform for *E. histolytica* included that it is an anaerobe and that no rapid readout assay is available. These issues have been solved by the use of GasPak™ EZ Anaerobe Gas Generating Pouch Systems (VWR) and CellTiter-Glo Luminescent Cell Viability Assay (Promega). The GasPak was not needed during robotic transfers, making this assay fully compatible with workstation-based automation. The assay development was performed with exponentially growing *E. histolytica* trophozoites with 50,000 parasites mL<sup>-1</sup> in 96-well<sup>8</sup> or 15,000 mL<sup>-1</sup> in 384-well microtiter plates. Anaerobic conditions were maintained using GasPak during growth. As ATP is an essential cofactor for biogenesis in *E. histolytica*, we used the luciferase-based assay to validate the correlation between the number of viable trophozoites and their ATP levels. The relationship between numbers of parasites seeded into 96- and 384-well plates and relative luminescence from CellTiter-Glo of parasites showed a linear correlation ( $R^2 = 0.86$  and  $R^2 = 0.9$ ) (Fig. 1a,b). Trophozoites readily tolerated up to 0.5% DMSO with no effect on growth rate. In our system, the EC<sub>50</sub> value for metronidazole, defined as that concentration of compound necessary to reduce the culture density to 50% of that of a DMSO-treated culture, was 5 μM. This HTS assay was used to evaluate the amebicidal activity of chemicals to identify potential drug candidates and was performed with 50,000 parasites mL<sup>-1</sup> in 96-well microtiter plate at a single concentration of 5 μM.

The screen was performed with a 910-member Iconix library, consisting of both FDA-approved and unapproved bioactive compounds. The use of drugs already approved for human use opens the possibility to rapidly and cost-effectively reprofile or repurpose<sup>9</sup> drugs to treat amebiasis. This offers shortened development timelines and decreased risk with compounds having already passed regulatory clinical trials with full toxicological and pharmacokinetic profiles<sup>9</sup>.

Eleven compounds were identified as “active,” causing statistically significant growth inhibition (> 50%; Fig. 1c and Table 1). The assay showed excellent discrimination between active and inactive compounds with a  $Z'$  factor of  $0.96 \pm 0.13$  in the screening experiment using 12 different plates. Among 11 compounds, auranofin demonstrated the highest amebicidal activity with an EC<sub>50</sub> of 0.5 μM, 10-fold better than the current drug of choice, metronidazole. Repurchased auranofin and three auranofin analogs also inhibited growth of *E. histolytica* trophozoites (Supplementary Table 1). Two purine analogs, cladribine and fludarabine, showed 79% and 77% inhibition at 5 μM, respectively, but are not promising for further development because of reported adverse effects on patients. Trifluoperazine, a compound with known amebicidal activity<sup>10</sup> was also identified as a primary hit, confirming the sensitivity of our whole cell HTS assay format.

Auranofin is an FDA-approved oral, gold-containing drug that has been in clinical use to treat rheumatoid arthritis (RA) for 25 years and is sold as Ridaura™ (Prometheus Laboratories). The published pharmacokinetic data of auranofin comes from studies in RA patients following long-term therapy. Auranofin is rapidly metabolized so no intact drug can be detected, but gold levels have been measured. Following an oral dose, 25% of auranofin is absorbed, 60% is plasma protein bound, and 85% excreted in feces<sup>11</sup>. Steady-state mean blood gold levels are  $0.68 \pm 0.45 \mu\text{g mL}^{-1}$  (package insert) or approximately  $3.5 \mu\text{M}$ , more than seven times the  $\text{EC}_{50}$  for *E. histolytica*. Auranofin was approved for the long-term treatment of unresponsive RA with courses for a minimum of 6 months at doses of 3 mg once or twice a day. The complications listed in the package insert for long-term (> 1 yr) auranofin therapy include dermatologic: rash (26%); gastrointestinal: loose stools (42%), abdominal pain (14%), nausea (10%); hematologic: anemia, leucopenia, thrombocytopenia in up to 3%; hepatic: elevated liver enzymes (2%); mucous membranes: stomatitis (13%); renal: proteinuria (1%). The likelihood of gold toxicity is extremely small in short-term (7–10 d) therapy for amebiasis.

Recently, auranofin has been shown to rapidly kill juvenile and adult *Schistosoma mansoni* in culture at physiological concentrations ( $5 \mu\text{M}$ )<sup>12</sup>, as well as bloodstream and procyclic stages of *Trypanosoma brucei*<sup>13</sup>. Concentrations as low as  $2.5 \mu\text{M}$  also killed larval worms of *Echinococcus granulosus*<sup>14</sup>. Auranofin also strongly inhibited the growth of malarial parasite *Plasmodium falciparum in vitro*<sup>15</sup> and killed the promastigote stage of *Leishmania infantum* at micromolar concentration<sup>16</sup>.

Despite 25 years of clinical use, the mechanism of action of auranofin is poorly understood. To identify the basis of auranofin activity versus *E. histolytica*, a transcriptional profiling study was undertaken using *E. histolytica* oligonucleotide microarrays<sup>17</sup>. Incubation of *E. histolytica* with auranofin for only 3 h at  $1 \mu\text{M}$  concentration identified auranofin-induced downregulation of critical genes involved in mitosis (Rae1<sup>18</sup>) and nucleotide metabolism (nucleoside diphosphate kinase<sup>19</sup>), while signal transduction genes encoding ADP-ribosylation factor and Ras1p were upregulated<sup>20</sup> (Supplementary Table 2). However, these transcripts are also induced by other forms of cellular stress. Furthermore, there was a marked upregulation of the gene encoding a protein similar to arsenite-inducible RNA-associated protein (AIRAP) (Supplementary Table 2). The differential expressions of these transcripts were validated by quantitative real-time PCR (qRT-PCR) (Supplementary Fig. 1 and Supplementary Table 3).

AIRAP is unique among known arsenite-induced genes in that expression is not upregulated in response to other oxidants and is only modestly induced by exposure to other metals, such as zinc<sup>21</sup>. We have shown that the transcript for a gene similar to AIRAP in *E. histolytica* was highly upregulated by treatment with low concentrations of auranofin, thereby identifying a novel gene in *E. histolytica* selectively inducible by auranofin exposure. It is noteworthy that both arsenite and auranofin are reported to be inhibitors of thioredoxin reductase (TrxR)<sup>22,23</sup> and metabolic inhibitors of selenium metabolism<sup>24</sup>. This led us to hypothesize that *E. histolytica* TrxR likely is the target for auranofin. Because *E. histolytica* resides in either aerobic (liver) or anaerobic environments (colon) in their mammalian hosts, they must have means to minimize damage caused by reactive oxygen species produced by

the host immune assault. In most organisms there are two largely independent systems to detoxify reactive oxygen species, one based on glutathione and the other based on thioredoxin. Each of these systems has a dedicated NADPH-dependent flavoenzyme, glutathione reductase and TrxR, to maintain the reduced state of glutathione or thioredoxin, respectively<sup>25-7</sup>. However, *E. histolytica* lacks both glutathione reductase activity and glutathione synthetic enzymes<sup>28</sup>; its TrxR is involved in prevention, intervention and repair of damage caused by oxidative stress<sup>29</sup>.

There is a single TrxR-encoding gene in the *E. histolytica* genome (23.m00296), which belongs to the low molecular weight TrxR family<sup>30</sup>, and is similar to bacterial and yeast enzymes, including the TrxR from *Escherichia coli* (Supplementary Fig. 2). In contrast, most higher eukaryotes have a high molecular weight TrxR which is typically a selenocysteine protein; this enzyme in *S. mansoni*, known as TGR, has both Se and an appended glutaredoxin domain<sup>23</sup> (Supplementary Fig. 3). We hypothesized that *EhTrxR* would not contain selenium and that auranofin would bind to the active site cysteines. Active, His-tagged *EhTrxR* was readily purified from solubilized *E. coli* by nickel-affinity chromatography, with properties similar to those previously reported for *EhTrxR*<sup>29</sup>.

The activities of auranofin and its two most active analogs were examined for inhibition of recombinant *EhTrxR*. Low  $\mu\text{M}$  concentrations of auranofin and analog 39 and nM concentrations of analog 7 were inhibitory (Fig. 2a-c). The assays were non-linear for the first 50 s, unlike control reactions without auranofin; inhibition increased with time until a linear, inhibited rate was established after 50 s of reaction (Fig. 2a, **inset**). Examination of the rates after 50 s indicated that 0.4  $\mu\text{M}$  auranofin caused 50% inhibition. Preincubation of the inhibitor with reduced *EhTrxR* did not remove the lag phase in inhibition as seen by the nonlinearity of the data acquired up to 50 s (not shown).

Because TrxR is critical for protecting amebic trophozoites from oxidant attack, we compared the susceptibility of trophozoites with and without auranofin treatment to reactive oxygen species using  $\text{H}_2\text{O}_2$ . Following incubation of trophozoites with 2  $\mu\text{M}$  auranofin for 18 h, the remaining viable trophozoites (~50%) were significantly more sensitive to killing by 300  $\mu\text{M}$   $\text{H}_2\text{O}_2$  than control trophozoites in media alone ( $P < 0.002$ ) (Fig. 2d). Killing by auranofin (2  $\mu\text{M}$ ) and  $\text{H}_2\text{O}_2$  was reversed by the presence of 2  $\text{mg mL}^{-1}$  of cysteine (Fig. 2d). Cysteine is the major reductant in the trophozoite<sup>31</sup>, and its apparent protective effect may be through direct reduction of thioredoxin or inhibition of auranofin binding to cysteine residues in TrxR. The presence of reactive oxygen species due to 2  $\mu\text{M}$  auranofin treatment could be detected with fluorescence generated by the oxidation of dichlorodihydrofluorescein<sup>32</sup> (Fig. 2e). However, the same concentration of metronidazole, although producing stress, did not increase intracellular reactive oxygen species (Supplementary Fig. 4). Moreover, increased oxidized thioredoxin was observed in auranofin-treated trophozoites, both *in vitro* and *in vivo*, indicating that TrxR likely is a target for auranofin (Fig. 2f).

Recently, Angelucci *et al*<sup>23</sup>, solved the crystal structure of *S. mansoni* TGR that had been incubated with auranofin before crystallization. The structure revealed gold [Au(I)] rather than auranofin as an adduct between pairs of cysteines (Cys-gold-Cys) in two different sites

and also bound to the proposed NADPH binding site of the reductase in a third location. The C-terminus of TGR containing a selenocysteine residue was not observed in the structure and may have bound a fourth gold atom. Angelucci *et al*<sup>23</sup> proposed that the selenocysteine at the penultimate position of TGR accelerated the release of gold from auranofin to form the inactivated enzymes; benzeneselenol added to a C-terminally truncated TGR or to glutathione reductase increased the rate of inactivation by auranofin. The crystal structure of reduced *L. infantum* trypanothione reductase in complex with NADPH and auranofin also demonstrated that gold binds to two active cysteine residues of trypanothione reductase<sup>16</sup>.

*EhTrxR* is of very similar size and domain topology as *E. coli* TrxR, a well-studied enzyme<sup>33</sup>. Both proteins have an active site dithiol/disulfide center (CATC for *EcTrxR*, CAIC for *EhTrxR*) plus either two or four additional Cys residues, respectively (Supplementary Fig. 2). By analogy with the *S. mansoni* TGR, addition of auranofin could cause gold atoms to bind to the NADPH-binding site of *EhTrxR*, to the active site thiols, to the four Cys residues near the C-terminus of the enzyme, or to some combination of these sites.

Because of auranofin's *in vitro* activity against *E. histolytica* trophozoites and oral availability, we tested its efficacy in two animal models of amebiasis. We adapted a murine amebic colitis model, in which trophozoites invade and colonize mouse cecal tissue following surgical inoculation<sup>34,35</sup>. Amebic trophozoites were co-cultured with cecal bacteria and surgically inoculated into the cecum of C3H/HeJ mice. Auranofin or metronidazole were delivered by gavage 24 h after infection at a concentration of 1 mg kg<sup>-1</sup> d<sup>-1</sup> for 7 d<sup>36</sup>. Both the parasite burden and the inflammatory response as measured by myeloperoxidase were significantly reduced by auranofin ( $P = 0.037$  and 0.0021) (Fig. 3a,b) but not by metronidazole (Fig. 3c,d). Auranofin (Fig. 3e) was more effective than an equivalent dose of metronidazole (Fig. 3f) in a hamster model of amebic liver abscess where treatment started 4 d after infection. A single oral dose of 3 mg kg<sup>-1</sup> d<sup>-1</sup> of auranofin for 7 d significantly decreased hepatic damage in hamsters ( $P = 0.002$ ) (Fig. 3e). These findings suggest that auranofin may be an entirely new class of drug to treat amebiasis and potentially other parasitic infections. Based on these results, the USFDA has approved an Orphan-Drug designation of auranofin for treatment of amebiasis.

In summary, we have shown that it is feasible to screen large numbers of compounds in an HTS-format versus *E. histolytica* and robust and reproducible results can be generated from this HTS. The discovery of the amebicidal activity of the FDA-approved drug auranofin and its recent orphan-drug designation offer a promising drug repositioning opportunity for the treatment of amebiasis.

## METHODS

### *E. histolytica* cultures

Axenic *E. histolytica* (HM1:IMSS) trophozoites were maintained in TYI-S-33 medium<sup>38</sup> and counted using a particle counter (Beckman Coulter).

## Compound libraries

A library of 910 bioactive compounds was donated by Iconix Biosciences.

## HTS cell viability assay

Compounds were diluted using a Biomek FX<sup>P</sup> Laboratory Automation Workstation (Beckman Coulter) and the Matrix WellMate bulk dispenser (Thermo Fisher Scientific) to yield 125  $\mu\text{M}$  compound in 12.5% DMSO. Finally, FX<sup>P</sup> transferred 4  $\mu\text{L}$  of diluted compound to the 96-well screen plates, followed by addition of 96  $\mu\text{L}$  (5,000 parasites) of *E. histolytica* trophozoites in TYI-S-33 complete medium to the 96-well plates, by the WellMate. Final concentrations of test compound and DMSO per well were 5  $\mu\text{M}$  and 0.5%, respectively.

Negative controls in the screen plates contained 0.5% DMSO and positive controls contained 30  $\mu\text{M}$  metronidazole (Sigma). Assay plates were incubated for 48 h at 37 °C in the GasPak to maintain an anaerobic condition throughout the incubation period. At the end of incubation, the assay plates were equilibrated to room temp. for 30 min, 50  $\mu\text{L}$  of CellTiter-Glo were added in each well of the 96-well plates, using the WellMate. The plates were then placed on an orbital shaker at RT for 10 min to induce cell lysis. After lysis, the plates were again equilibrated at RT for 10 min to stabilize the luminescent signal. The resulting ATP-bioluminescence of the trophozoites was measured at RT using an Analyst HT plate reader (Molecular Devices).

## Secondary screen for potency determination

For confirmatory screens of trophozoites, hits from the primary screen were picked from 5 mM stocks in 100% DMSO using the Biomek FX<sup>P</sup>. For 8-point EC<sub>50</sub> determination experiments, we diluted 2.5  $\mu\text{L}$  of stock compounds with 17.5  $\mu\text{L}$  sterile water to yield 625  $\mu\text{M}$  working concentration of library compounds. A three-fold serial dilution was then performed yielding a concentration range 0.25–625  $\mu\text{M}$ . From this dilution plate, 4  $\mu\text{L}$  were transferred into the 96-well screen plates followed by addition of 96  $\mu\text{L}$  of trophozoites (5,000 parasites) to yield a final 8-point concentration range spanning 0.01–25  $\mu\text{M}$  in final 0.5% DMSO. The assays were performed in triplicate using CellTiter-Glo. Visualization and statistical analysis of secondary screening were performed using GraphPad Prism software 4.0.

## HTS data analysis and statistics

The raw data file from the Analyst HT plate reader was uploaded using Pipeline Pilot 4.5.2 into Small Molecule Discovery Center's database (MySQL). The results are posted (<http://smdc.ucsf.edu/hits/>) with tables, Z', heat maps, scatter plots, and percent inhibition relative to maximum and minimum reference signal controls. Percent inhibition relative to maximum and minimum reference signal controls was calculated using the formula:

$$\% \text{ Inhibition} = \left[ \frac{\text{mean of Maximum Signal Reference Control} - \text{Experimental Value}}{\text{mean of Maximum Signal Reference Control} - \text{mean of Minimum Signal Reference Control}} \right] \times 100$$

The cutoff was selected to determine actives from the primary screen, which was at least 50% inhibition and 3 standard deviations above the mean of the population of compounds tested.

### ***E. histolytica* microarray analysis**

We used *E. histolytica* oligonucleotide arrays for characterizing transcriptional effects of auranofin. These microarrays were composed of 6209, 70 mer oligonucleotides and encompassed approximately 90% of the unique genes found in the *E. histolytica* genome dataset as of February 2004. Oligonucleotides were printed in triplicate on slides by the Washington University School of Medicine Microarray Core Facility<sup>17</sup>. We isolated total RNA from 3 h 0.5% DMSO-treated  $2 \times 10^6$  *E. histolytica* HM1:IMSS and 3 h 1  $\mu$ M auranofin-treated  $2 \times 10^6$  HM1 using TRIZOL (Invitrogen). Total RNA was amplified with the Amino Allyl MessageAmp™ II aRNA Amplification Kit (Ambion) following the manufacturer's protocol. The monofunctional NHS-ester Cy3 and Cy5 dyes (GE Healthcare Life Sciences) were coupled with 10  $\mu$ g amplified RNA. The two aRNA pools to be compared were mixed and applied to *E. histolytica* microarray. Four samples (two from DMSO-treated and two from auranofin-treated) were competitively hybridized on two individual chips. The hybridization was performed at 63 °C for 16 h in a humidified slide chamber containing the labeled probe, 3X SSC, and 0.2% SDS. After hybridization, the hybridization chamber was removed from the 63 °C water bath, washed with 0.6X SSC, 0.03% SDS, and then 0.06X SSC. Microarrays were scanned using a GenePix Pro Axon 4000B scanner, data were analyzed (Acuity software, Molecular Devices) and deposited in the public database ArrayExpress (<http://www.ebi.ac.uk/arrayexpress>) under the accession number E-MEXP-3494.

### **qRT-PCR**

We isolated total RNA from control and auranofin-treated trophozoites (above). After reverse transcription, we performed qRT-PCR using SYBR Green I Master (Roche Applied Science) and the PCR product was monitored (Mx3005P™ QPCR System with MxPro™ QPCR software, Stratagene). Primer sequences are in Supplementary Table 3.

### **Purification of recombinant *E. histolytica* TrxR**

The *Eh*TrxR coding sequence was amplified<sup>29</sup> from genomic DNA<sup>35</sup>, cloned into pET22b (Novagen) and transformed into BL21 Codon Plus cells (Stratagene). Protein expression was induced (1 mM IPTG, 2 h, 37 °C), the pellet lysed in B-PER (Thermo Scientific), and soluble *Eh*TrxR (1% Triton X-100, 10 mM imidazole) purified by NiNTA affinity chromatography (Qiagen).

### ***E. histolytica* TrxR assay**

The thionitrobenzoate-coupled assay for TrxR activity was modified from Mulrooney<sup>39</sup>. Briefly, 600  $\mu$ L total of 50 mM potassium phosphate, pH 7.0, 1 mM EDTA contained 20  $\mu$ M *E. coli* Trx1, 200  $\mu$ M 5,5'-dithiobis(2-nitrobenzoic acid) (DTNB) and 20 or 45 nM *Eh*TrxR at 25 °C. The reaction was started by addition of 100  $\mu$ M NADPH and monitored by 412 nm absorbance, which increases with reaction due to DTNB reduction. With these

concentrations of DTNB and *Eh*TrxR, in the absence of *Ec*TrxA there was a negligible increase in 412 nm absorbance. When present, the indicated concentration of auranofin (predissolved in ethanol) was added 3 minutes before the NADPH (to a maximum added volume, at 3.6  $\mu$ L, of 0.6% of the total). The initial rate and the rate after 50 s were calculated from the increase in 412 nm absorbance, using an extinction coefficient for nitrothiobenzoate anion of 13,600  $M^{-1} cm^{-1}$  (with 2 molecules of nitrothiobenzoate generated per NADPH oxidized) to convert the absorbance change to rates in nmol NADPH  $min^{-1}$ .

### Auranofin effect on trophozoites

To determine the effect of auranofin on oxidant stress, we pre-incubated trophozoites ( $5 \times 10^5$  in TYI-S-33) at 37 °C with auranofin (2  $\mu$ M, 18 h), ethanol, or TYI-S-33 containing 2 mg  $mL^{-1}$  of cysteine (Sigma). Trophozoites were then counted, viability assessed by trypan blue exclusion, and resuspended in TYI-S-33 with 300  $\mu$ M  $H_2O_2$ . Aliquots were removed in triplicate every 30 min for 2 h and % survival determined with the CellTiter-Glo with statistical analysis by Student's *t* test.

We determined intracellular oxidant levels incubating control (ethanol), ethanol +  $H_2O_2^-$ , auranofin-, and auranofin +  $H_2O_2^-$ -treated trophozoites with 0.2 mM 2',7'-dichlorodihydrofluorescein diacetate (Sigma) for 45 min<sup>32</sup>, washing, fixing with 4% paraformaldehyde, resuspending in ProLong Gold mounting media with nuclear stain (DAPI) and examining by a Nikon E800 fluorescence microscope.

The redox state of thioredoxin in amebic trophozoites was determined by protein electrophoretic mobility shift assay<sup>37</sup>. HM-1 trophozoites were incubated 18 h with auranofin (2  $\mu$ M) or media alone. *In vivo* trophozoites were obtained by flushing infected mice cecum after treatment for 48 h with auranofin at 1 mg  $kg^{-1}$  or the ethanol vehicle alone. Trophozoites were washed in PBS, pH 7.4, lysed in 100 mM Tris, 8 M urea, 1 mM EDTA and 30 mM iodoacetic acid, pH 7.2 for 37 °C for 15 min., excess IAA removed by precipitation in cold acetone/1 N HCl (98:2, v/v) and washed in acetone/1 N HCl, water (98:2:10). The disulfides were subsequently reduced in the urea buffer containing 3.5 mM DTT for 30 min at 37 °C, and the new thiols amidomethylated with 10 mM iodoacetamide. Markers were prepared by incubating cultured trophozoites in urea buffer with 3.5 mM DTT for 30 min at 37 °C, then equal aliquots alkylated with 30 mM iodoacetic acid (reduced marker) or 10 mM iodoacetamide (oxidized) marker for 30 min at 37 °C<sup>37</sup>. Samples were electrophoresed by native urea-PAGE on 9% gels, transferred to nitrocellulose and the bands detected with rabbit *Eh*Trx-specific antibody<sup>29</sup> (1:200) and goat anti-rabbit horseradish peroxidase (Invitrogen, 1:10,000) by enhanced chemiluminescence (SuperSignal, West Pico, Fisher Scientific).

### *In vivo* efficacy of auranofin

We injected cecal-passed trophozoites into the externalized cecum of six-week-old C3H/HeJ male mice<sup>34</sup> (The Jackson Laboratory) and treated orally 24 h after infection with 1 mg  $kg^{-1} d^{-1}$  auranofin (Enzo Life Sciences) or metronidazole for 7 d. The mice were then sacrificed, the cecum removed for histopathology, quantification of trophozoites by real-time PCR, and



myeloperoxidase (MPO) activity<sup>40</sup>. Mouse studies were approved by the UCSD Institutional Animal Care Committee.

We injected trophozoites (250,000 in 0.2 mL TYI-S-33) intraperitoneally in hamsters to induce liver abscesses. The hamsters were treated 4 d after infection orally with 3 mg kg<sup>-1</sup> of auranofin, metronidazole, or PBS daily for 7 d. The hamsters were sacrificed and the livers and abscesses were dissected and weighed. Hamster studies were approved by the CINVESTAV-IPN Internal Committee for the Care and Use of the Laboratory Animals.

## Supplementary Material

Refer to Web version on PubMed Central for supplementary material.

## ACKNOWLEDGMENTS

This work was supported by the Sandler Foundation and NIAID 5U01AI077822-02; support from R01 GM050389 is also acknowledged. *E. histolytica* microarray slides were kindly provided by S. L. Stanley Jr. of Stony Brook University, New York, and the *E. histolytica* thioredoxin-specific antibody a kind gift from S. Adrian-Guerrero of the Universidad Nacional del Litoral, Santa Fe, Argentina. We thank, G. Hwang and C. Le for their help with the animal surgery, and K. Ang and J. Gut for sharing their expertise.

## REFERENCES

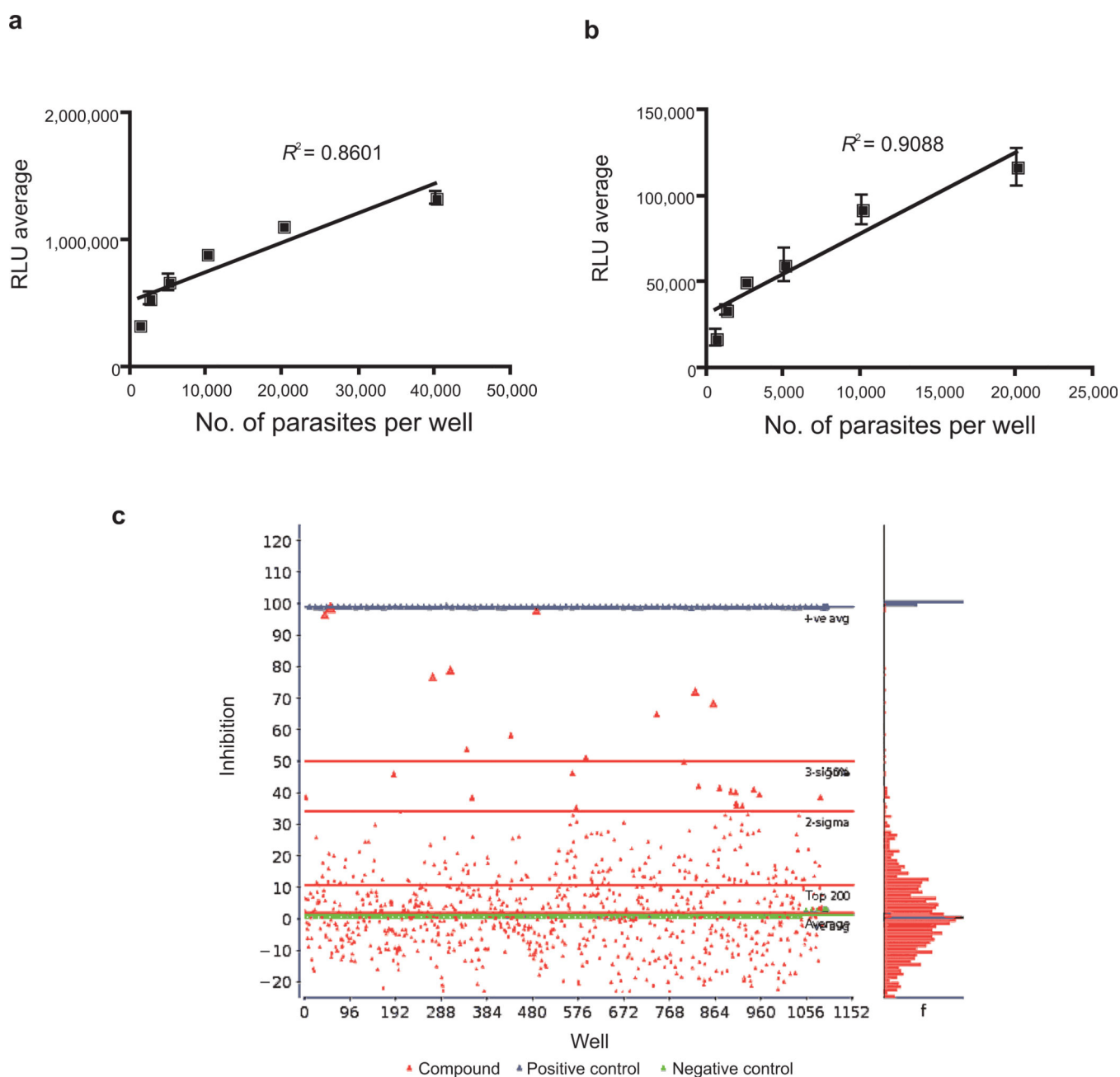
1. World Health Organization. Geneva: World Health Organization; 1998. The World Health Report 1998: life in the 21st century: a vision for all.
2. Freeman CD, Klutman NE, Lamp KC. Metronidazole. A therapeutic review and update. *Drugs*. 1997; 54:679–708. [PubMed: 9360057]
3. Krogstad, DJ.; Cedeno, JR. Problems with current therapeutic regimens. In: Ravdin, JI., editor. *Amebiasis: human infection by Entamoeba histolytica*. New York: John Wiley & Sons, Inc.; 1988. p. 741-748.
4. Samarawickrema NA, Brown DM, Upcroft JA, Thammapalerd N, Upcroft P. Involvement of superoxide dismutase and pyruvate:ferredoxin oxidoreductase in mechanisms of metronidazole resistance in *Entamoeba histolytica*. *J. Antimicrob. Chemother.* 1997; 40:833–840. [PubMed: 9462435]
5. Wassmann C, Hellberg A, Tannich E, Bruchhaus I. Metronidazole resistance in the protozoan parasite *Entamoeba histolytica* is associated with increased expression of iron-containing superoxide dismutase and peroxiredoxin and decreased expression of ferredoxin 1 and flavin reductase. *J. Biol. Chem.* 1999; 274:26051–26056. [PubMed: 10473552]
6. Seifert K, et al. Effects of miltefosine and other alkylphosphocholines on human intestinal parasite *Entamoeba histolytica*. *Antimicrob. Agents Chemother.* 2001; 45:1505–1510. [PubMed: 11302818]
7. Ghosh S, et al. Effects of bisphosphonates on the growth of *Entamoeba histolytica* and *Plasmodium* species *in vitro* and *in vivo*. *J. Med. Chem.* 2004; 47:175–187. [PubMed: 14695831]
8. Singh S, Athar F, Azam A. Synthesis, spectral studies and *in vitro* assessment for antiamebic activity of new cyclooctadiene ruthenium(II) complexes with 5-nitrothiophene-2-carboxaldehyde thiosemicarbazones. *Bioorg. Med. Chem. Lett.* 2005; 15:5424–5428. [PubMed: 16213728]
9. Ashburn TT, Thor KB. Drug repositioning: identifying and developing new uses for existing drugs. *Nat. Rev. Drug Discov.* 2004; 3:673–683. [PubMed: 15286734]
10. Makioka A, Kumagai M, Ohtomo H, Kobayashi S, Takeuchi T. Effect of calcium antagonists, calcium channel blockers and calmodulin inhibitors on the growth and encystation of *Entamoeba histolytica* and *E. invadens*. *Parasitol. Res.* 2001; 87:833–837. [PubMed: 11688889]
11. Gottlieb NL. Pharmacology of auranofin: overview and update. *Scand. J. Rheumatol. Suppl.* 1986; 63:19–28. [PubMed: 3110942]

12. Kuntz AN, et al. Thioredoxin glutathione reductase from *Schistosoma mansoni*: an essential parasite enzyme and a key drug target. *PLoS Med.* 2007; 4:e206. [PubMed: 17579510]
13. Lobanov AV, Gromer S, Salinas G, Gladyshev VN. Selenium metabolism in Trypanosoma: characterization of selenoproteomes and identification of a kinetoplastida-specific selenoprotein. *Nucl. Acids Res.* 2006; 34:4012–4024. [PubMed: 16914442]
14. Bonilla M, et al. Platyhelminth mitochondrial and cytosolic redox homeostasis is controlled by a single thioredoxin glutathione reductase and dependent on selenium and glutathione. *J. Biol. Chem.* 2008; 283:17898–17907. [PubMed: 18408002]
15. Sannella AR, et al. New uses for old drugs. Auranofin, a clinically established antiarthritic metallodrug, exhibits potent antimalarial effects *in vitro* : Mechanistic and pharmacological implications. *FEBS Lett.* 2008; 582:844–847. [PubMed: 18294965]
16. Ilari A, et al. A gold-containing drug against parasitic polyamine metabolism: the X-ray structure of trypanothione reductase from *Leishmania infantum* in complex with auranofin reveals a dual mechanism of enzyme inhibition. *Amino Acids.* 2012; 42:803–811. [PubMed: 21833767]
17. Davis PH, Schulze J, Stanley SL Jr. Transcriptomic comparison of two *Entamoeba histolytica* strains with defined virulence phenotypes identifies new virulence factor candidates and key differences in the expression patterns of cysteine proteases, lectin light chains, and calmodulin. *Mol. Biochem. Parasitol.* 2007; 151:118–128. [PubMed: 17141337]
18. Blower MD, Nachury M, Heald R, Weis K. A Rae1-containing ribonucleoprotein complex is required for mitotic spindle assembly. *Cell.* 2005; 121:223–234. [PubMed: 15851029]
19. Parks RE Jr. et al. Purine metabolism in primitive erythrocytes. *Comp. Biochem. Physiol. B.* 1973; 45:355–364. [PubMed: 4351428]
20. Crechet JB, Cool RH, Jacquet E, Lallemand JY. Characterization of *Saccharomyces cerevisiae* Ras1p and chimaeric constructs of Ras proteins reveals the hypervariable region and farnesylation as critical elements in the adenyl cyclase signaling pathway. *Biochemistry.* 2003; 42:14903–14912. [PubMed: 14674766]
21. Sok J, et al. Arsenite-inducible RNA-associated protein (AIRAP) protects cells from arsenite toxicity. *Cell Stress Chaperones.* 2001; 6:6–15. [PubMed: 11525245]
22. Lu J, Chew EH, Holmgren A. Targeting thioredoxin reductase is a basis for cancer therapy by arsenic trioxide. *Proc. Natl. Acad. Sci. U S A.* 2007; 104:12288–12293. [PubMed: 17640917]
23. Angelucci F, et al. Inhibition of *Schistosoma mansoni* thioredoxin-glutathione reductase by auranofin: structural and kinetic aspects. *J. Biol. Chem.* 2009; 284:28977–28985. [PubMed: 19710012]
24. Talbot S, Nelson R, Self WT. Arsenic trioxide and auranofin inhibit selenoprotein synthesis: implications for chemotherapy for acute promyelocytic leukaemia. *Br. J. Pharmacol.* 2008; 154:940–948. [PubMed: 18587442]
25. Townsend DM, Tew KD, Tapiero H. The importance of glutathione in human disease. *Biomed. Pharmacother.* 2003; 57:145–155. [PubMed: 12818476]
26. Lillig CH, Holmgren A. Thioredoxin and related molecules—from biology to health and disease. *Antioxid. Redox. Signal.* 2007; 9:25–47. [PubMed: 17115886]
27. Sayed AA, et al. Identification of oxadiazoles as new drug leads for the control of schistosomiasis. *Nat. Med.* 2008; 14:407–412. [PubMed: 18345010]
28. Fahey RC, Newton GL, Arrick B, Overdank-Bogart T, Aley SB. *Entamoeba histolytica*: a eukaryote without glutathione metabolism. *Science.* 1984; 224:70–72. [PubMed: 6322306]
29. Arias DG, Gutierrez CE, Iglesias AA, Guerrero SA. Thioredoxin-linked metabolism in *Entamoeba histolytica*. *Free Radic. Biol. Med.* 2007; 42:1496–1505. [PubMed: 17448896]
30. Hirt RP, Muller S, Embley TM, Coombs GH. The diversity and evolution of thioredoxin reductase: new perspectives. *Trends Parasitol.* 2002; 18:302–308. [PubMed: 12379950]
31. Jeelani G, et al. Two atypical L-cysteine-regulated NADPH-dependent oxidoreductases involved in redox maintenance, L-cystine and iron reduction and metronidazole activation in the enteric protozoan *Entamoeba histolytica*. *J. Biol. Chem.* 2010; 285:26889–26899. [PubMed: 20592025]
32. Sen A, Chatterjee NS, Akbar MA, Nandi N, Das P. The 29-kilodalton thiol-dependent peroxidase of *Entamoeba histolytica* is a factor involved in pathogenesis and survival of the parasite during oxidative stress. *Euk. Cell.* 2007; 6:664–673.

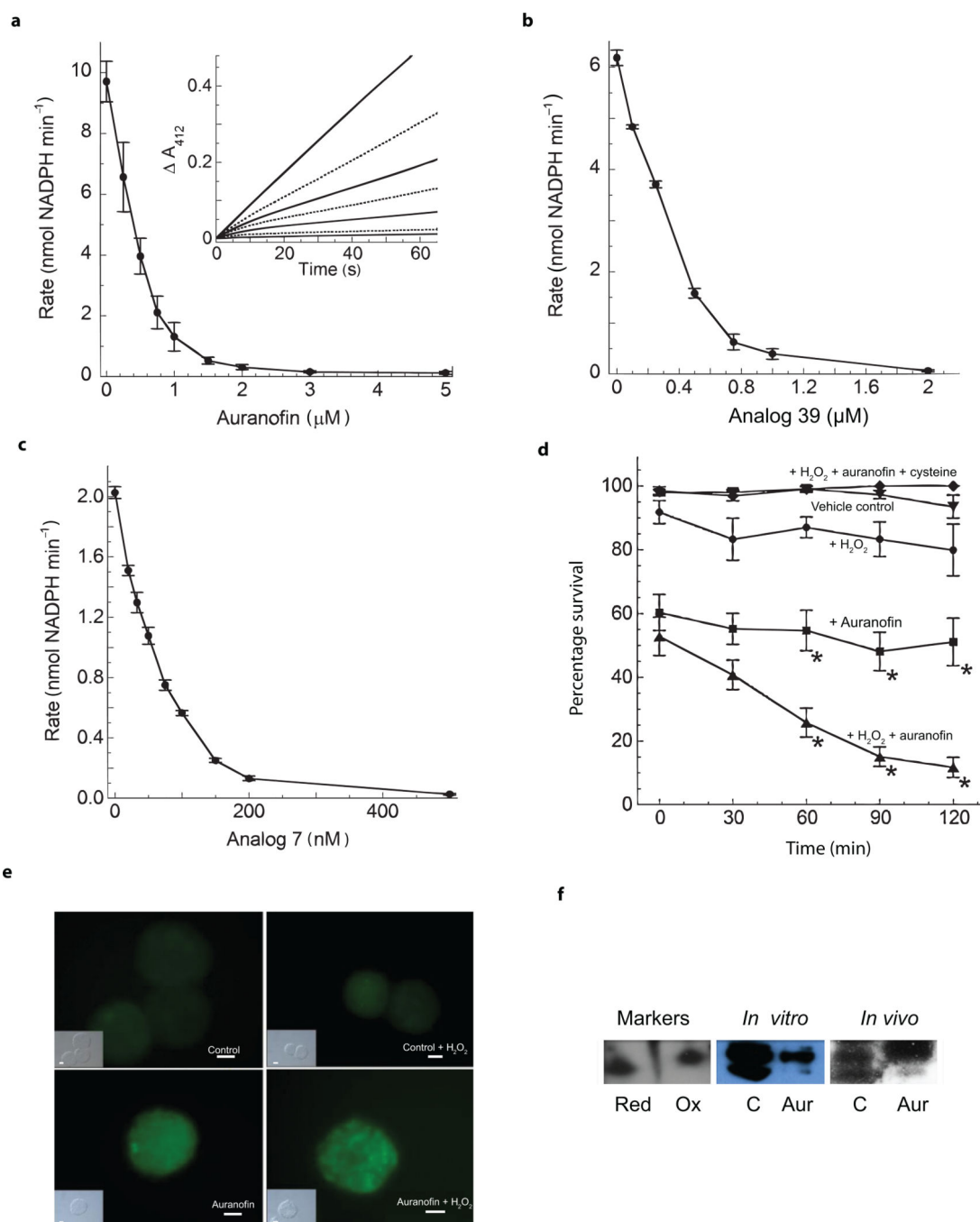
33. Williams CH, et al. Thioredoxin reductase: two modes of catalysis have evolved. *Eur. J. Biochem.* 2000; 267:6110–6117. [PubMed: 11012662]
34. Houpt ER, et al. The mouse model of amebic colitis reveals mouse strain susceptibility to infection and exacerbation of disease by CD4+ T cells. *J. Immunol.* 2002; 169:4496–4503. [PubMed: 12370386]
35. He C, et al. A novel *Entamoeba histolytica* cysteine proteinase, EhCP4, is key for invasive amebiasis and a therapeutic target. *J. Biol. Chem.* 2010; 285:18516–18527. [PubMed: 20378535]
36. Markiewicz VR, Saunders LA, Geus RJ, Payne BJ, Hook JB. Carcinogenicity study of auranofin, an orally administered gold compound in mice. *Fundam. Appl. Toxicol.* 1988; 11:277–284. [PubMed: 3220206]
37. Bersani NA, Merwin JR, Lopez MI, Pearson GD, Merrill GF. Protein electrophoretic mobility shift assay to monitor redox state of thioredoxin in cells. *Meth. Enzymol.* 2002; 347:317–326. [PubMed: 11898422]

## References for methods

38. Diamond LS, Harlow DR, Cunnick CC. A new medium for the axenic cultivation of *Entamoeba histolytica* and other *Entamoeba*. *Trans. R Soc. Trop. Med. Hyg.* 1978; 72:431–432. [PubMed: 212851]
39. Mulrooney SB. Application of a single-plasmid vector for mutagenesis and high-level expression of thioredoxin reductase and its use to examine flavin cofactor incorporation. *Protein Expr. Purif.* 1997; 9:372–378. [PubMed: 9126609]
40. Melendez-Lopez SG, et al. Use of recombinant *Entamoeba histolytica* cysteine proteinase 1 to identify a potent inhibitor of amebic invasion in a human colonic model. *Euk. Cell.* 2007; 6:1130–1136.



**Figure 1.** Assay development for HTS and scatter plot of percentage inhibition of each well from plates of compound library. **(a)** Correlation between the number of viable *E. histolytica* trophozoites and ATP-bioluminescence in 96-well microtiter plate. **(b)** Correlation between the number of viable *E. histolytica* trophozoites and ATP-bioluminescence in 384-well microtiter plate. Values plotted **(a,b)** are the means and standard deviations of triplicate wells. Line **(a,b)** represents the linear regression for plotted data. **(c)** Scatter plot of percentage inhibition of each well from twelve 96-well plates of the Iconix library. Eleven compounds yielded both 50% inhibition and 3 standard deviations above the mean of the population of compounds tested in the primary screen at 5  $\mu$ M.

**Figure 2.**

Inhibition of *EhTrxR* by auranofin and its analogs. The indicated concentrations of auranofin and analogs were incubated with 45 nM (**a,b**) or 20 nM *EhTrxR* (**c**), 20  $\mu$ M *E. coli* Trx1 and 200  $\mu$ M DTNB for 3 min before addition of NADPH to initiate the assay. With no auranofin or analogs added, there was a linear increase in absorbance over several minutes, whereas addition of auranofin and analogs resulted in a non-linear increase in absorbance over the first 50 s of reaction (shown for auranofin in the inset of **a**), at concentrations of 0, 0.25, 0.5, 0.75, 1, 2 and 5  $\mu$ M, in order of decreasing slope). The main plots show the final

linear rates of reaction after 50 s at each auranofin (**a**) and analog 39 (**b**) concentration. For analog 7, rate after 200 s of reaction was plotted (**c**). The plotted rates are the mean  $\pm$  S.E. of at least 3 determinations. The EC<sub>50</sub> values for auranofin, analog 39 and analog 7 were 0.4, 0.33 and 0.055  $\mu$ M, respectively. (**d**) Treatment of trophozoites with auranofin (2  $\mu$ M, 18 h) increases susceptibility to H<sub>2</sub>O<sub>2</sub> (300  $\mu$ M), but is reversed by cysteine at 2 mg mL<sup>-1</sup>. Time points represent the mean  $\pm$  S.E. of three experiments in triplicate. \*  $P < 0.002$  by Student's t test. (**e**) Reactive oxygen species are detected within trophozoites following treatment with 2  $\mu$ M auranofin (18 h) and 300  $\mu$ M H<sub>2</sub>O<sub>2</sub> (2 h) by fluorescence of dichlorofluorescein. Control trophozoites were treated with ethanol alone and ethanol  $\pm$  H<sub>2</sub>O<sub>2</sub>. Scale bars 10  $\mu$ m. (**f**) Auranofin treatment (Aur) increases oxidized (Ox) vs. reduced (Red) thioredoxin compared to controls (C) in *in vitro* and *in vivo* trophozoites detected by mobility shift assays<sup>37</sup>. Trophozoite standard markers depict completely reduced (Red-EhTrx<sup>SH</sup>) and completely oxidized (Ox-EhTrx<sup>SS</sup>) thioredoxin.

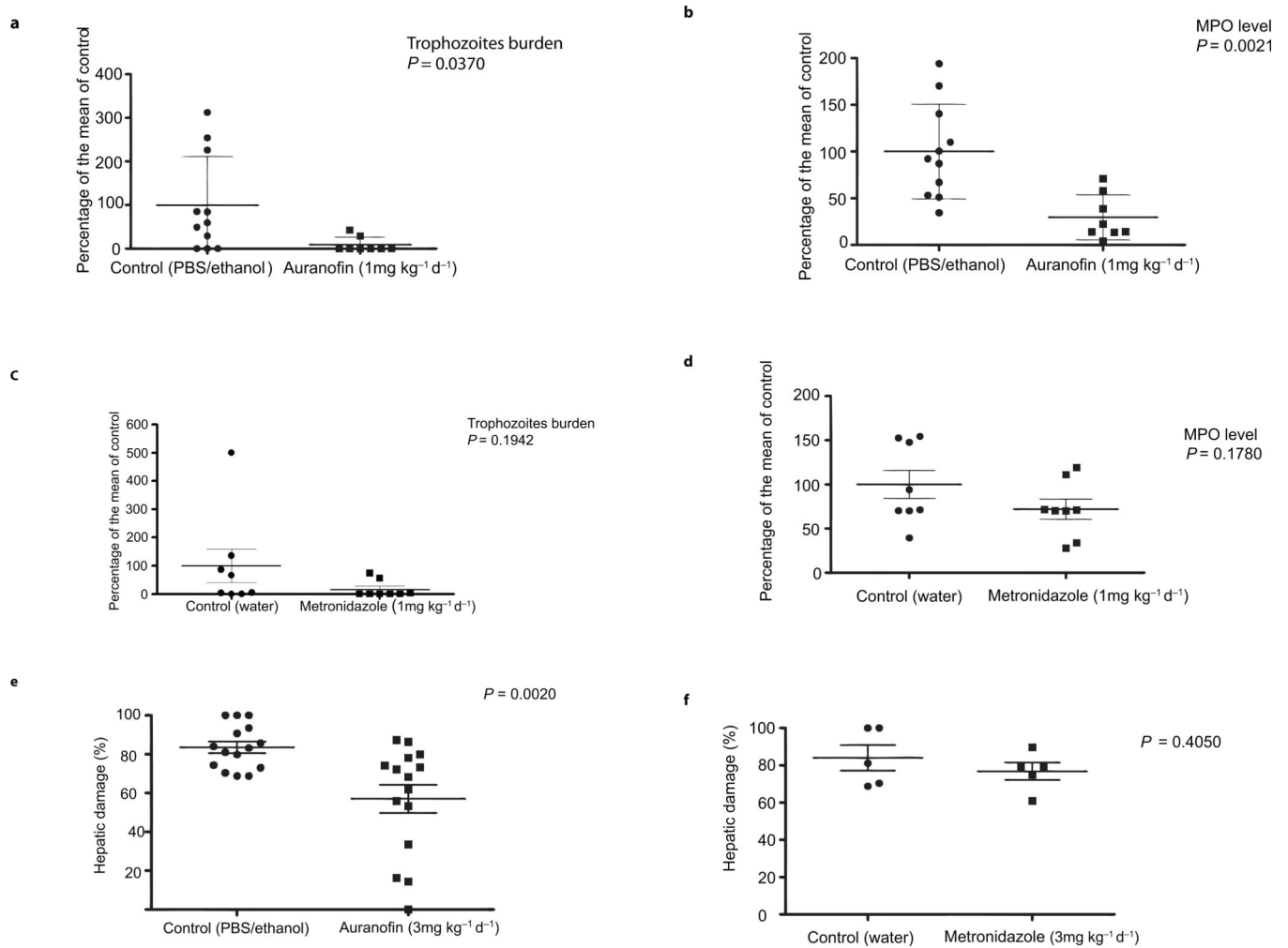


**Figure 3.** Effect of auranofin or metronidazole on animal models of amebic colitis and liver abscesses. The treatment of mice with cecal amebiasis with auranofin (**a,b**) or metronidazole (**c,d**) is presented as the percentage of trophozoites  $\text{gm}^{-1}$  of tissue or myeloperoxidase (MPO) units  $\text{gm}^{-1}$  of tissue compared with the means of infected controls (as 100%). Treatment of hamsters with auranofin (**e**) or metronidazole (**f**) for amebic liver abscess is presented as the percentage of hepatic damage, calculated as the weight of the abscess compared with the total liver weight before abscess removal (as 100%).

**Table 1**

Hits obtained after screening the Iconix library

<b>Compound</b>	<b>% Inhibition (5 <math>\mu</math>M)</b>
Auranofin	100
Sporidesmin A	99
Cycloheximide	98
Cladribine	79
Fludarabine	77
Homochlorcyclizine	73
Trifluoperazine	69
Idarubicin	65
4,4'-Diethylaminoethoxyhexestrol	58
Clomiphene	54
Amiodarone	51

Author Manuscript

Author Manuscript

Author Manuscript

Author Manuscript